Talanta 235 (2021) 122744

Contents lists available at ScienceDirect

Talanta

journal homepage: www.elsevier.com/locate/talanta

Ultrasensitive electrochemical detection of miRNA based on polymerization signal amplification

Qingyu Wang [a,c], Haobo Sun [a], Dongxiao Wen [b], Lei Wang [c], Lianzhi Li [c,**], Jinming Kong [a,*], Xueji Zhang [d]

[a] School of Environmental and Biological Engineering, Nanjing University of Science and Technology, Nanjing, 210094, PR China
[b] School of Chemistry and Chemical Engineering, Huazhong University of Science and Technology, Wuhan, 430074, PR China
[c] School of Chemistry and Chemical Engineering, Liaocheng University, Liaocheng, 252059, PR China
[d] School of Biomedical Engineering, Shenzhen University Health Science Center, Shenzhen, Guangdong, 518060, PR China

ARTICLE INFO

Keywords:
Electrochemical biosensor
ATRP
miRNA-141
Signal amplification

ABSTRACT

The detection of trace tumor-related serum miRNA biomarkers is in great demand for the early diagnosis of cancer. Herein, for the first time, an electrochemical sensing platform based on atom transfer radical polymerization (ATRP) signal amplification strategy for ultrasensitive determination of the breast and prostate cancer marker miRNA-141 has been developed. The hairpin DNAs were immobilized on the benzoic acid modified electrode to capture the target miRNA-141, the recognition of miRNA-141 released thiol groups on the end of probes, followed by the association of ATRP initiators modified gold nanoparticles with thiol groups, and then triggered the polymerization on electrode surface, causing a great number of ferrocene (Fc) signal molecules grafted on the sensor interface. As a result, the electrochemical signal intensity of signal molecule has been greatly increased. The proposed biosensor has a linear range from 10 pM to 10 aM with a detection limit of 3.23 aM for miRNA-141, opening a new and promising path for ultrasensitive analysis of tumor-related miRNAs.

1. Introduction

MicroRNAs (miRNAs) are single-stranded, short and nonprotein coding RNAs with approximately 19–23 nucleotides, and they are involved in a great deal of important processes of cell growth. Abnormal expression of miRNAs will lead to excessive growth, proliferation and differentiation of cells, and finally the occurrence of tumors [1,2]. Therefore, the presence of miRNA can be used for early cancer diagnosis due to its tumor specificity [3–5]. For instance, the abnormal expression of miRNA-141 has been proved to be closely associated with human breast and prostate cancers [6,7]. Thus, sensitive and accurate detection of miRNAs is very helpful for early detection and monitoring tumor biological process. However, due to miRNAs are easy degradation and small, it is difficult to make quantitative analysis of miRNAs [8].

Up to date, considerable approaches have been implemented to analyze miRNAs, such as northern blotting, reverse transcription polymerase chain reaction (RT-PCR) [1,2]. Unfortunately, these miRNA detection techniques have some intrinsic limitations, including low sensitivity or tedious sample preparation. Therefore, it is essential to develop a miRNA detection method featuring advantages of mild conditions, simple preparation, and easily available for clinical cancer diagnosis. In recent years, electrochemical method has received extensive attention due to its fast detection speed, high sensitivity, easy operation, and low cost. A variety of electrochemical sensors have been reported to sensitively detect miRNA-141 [9–13]. However, these sensors are mainly based on nanomaterials or DNAzyme for signal amplification, the sensitivity of these sensors is still unsatisfactory.

Recently, as one of the most important polymerization methods of controlled free radical polymerization (CRP), atom transfer radical polymerization (ATRP) has received extensive attention in the field of biosensing due to its advantages of simple operation, high efficiency, and low cost [14–17]. In ATRP signal amplification strategy, small signal monomer molecules are polymerized. Through chain growth, thousands of repeating units are associated, and the signal generated in the recognition process of the target biomolecule is amplified hundreds of times, realizing highly sensitive analysis of biomolecules. In addition,

* Corresponding author.
** Corresponding author.
E-mail addresses: lilianzhi@lcu.edu.can (L. Li), j.kong@njust.edu.cn (J. Kong).

https://doi.org/10.1016/j.talanta.2021.122744
Received 8 June 2021; Received in revised form 22 July 2021; Accepted 26 July 2021
Available online 28 July 2021

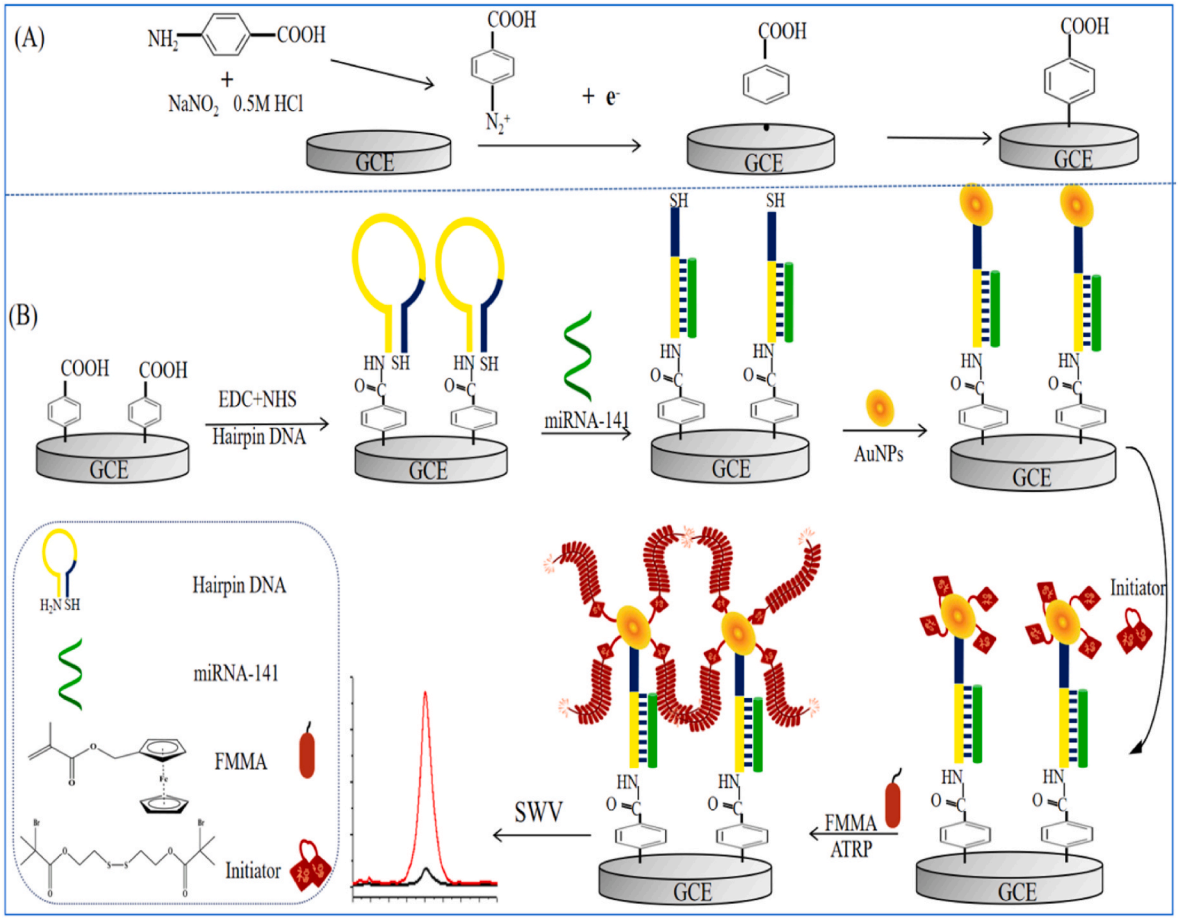

Scheme 1. ATRP signal amplification strategy for miRNA-141 detection.

ATRP has been an ideal choice in biosensing due to its mild reaction conditions and good adaptability to functional groups of biomacromolecules. Although ATRP signal amplification method has made significant progress in DNA and protein detection, the reports on miRNA biosensing is few [18], and no report on the application of ATRP signal amplification technology to electrochemical sensor for miRNA-141 sensitive detection yet.

In this paper, an ultrasensitive electrochemical biosensor based on ATRP signal amplification strategy for miRNA-141 analysis was established. Firstly, the hairpin DNAs were immobilized on the benzoic acid modified electrode, then the target miRNA-141 can be captured by hairpin DNAs. Next, gold nanoparticles (AuNPs) were connected to the sulfydryl of the opened hairpin DNAs through the Au–S bond. Subsequently, the initiators (the disulfide bond has been cleaved) were attached on AuNPs via the Au–S bond. Finally, the prepared electrodes were put in a solution containing monomer, catalyst and reductant to perform the activators generated by electron transfer for ATRP (AGET ATRP) reaction and generate a polymer containing a large number of Fc signal molecules. Therefore, the Fc electrochemical signal intensity was greatly amplified.

2. Experimental

2.1. Reagents and apparatus

The reagents and instruments have been described in detail in the *supplementary materials.*

2.2. The synthesis of AuNPs

The synthesis process of AuNPs was referred to the reported literature [19] and described in detail in the *supplementary materials.*

2.3. The biosensor preparation and electrochemical detection of miRNA-141

The detection principle was shown in Scheme 1. Firstly, $NaNO_2$ solution (10 mM, 10 mL) and *p*-aminobenzoic acid solution (20 mM, 10 mL) were prepared with 0.5 M HCL and deoxygenated with N_2 for 15 min, respectively. In an ice-water bath, $NaNO_2$ was slowly dropped into the *p*-aminobenzoic acid solution for diazotization reaction, 15 min later, diazonium salt was reduced to the GCE surface by cyclic voltammetry (CV), thus the benzoic acid modified GCE was prepared. Subsequently, the modified electrodes were activated by 200 μL EDC/NHS (40 mM/10 mM, pH 6.0 MES) solution for 30 min. After that, 10 μL hairpin DNA (0.1 μM, pH 7.4 PBS) was dropped onto the electrode surface and reacted with EDC/NHS at 37 °C for 2 h to obtain the hairpin DNA modified GCE, then the electrodes were incubated in different concentrations of miRNA-141 (pH 8.0, PBS buffer) for 2 h at 37 °C, the target miRNA-141 could be specifically recognized by the base complementary pairing and the hairpin DNA was opened. Then AuNPs were grafted to the end of hairpin DNAs via Au–S bond for 1 h at 37 °C. Next, the disulfide bond of ATRP initiator 2-[2-(2-bromo-2-methylpropanoyl)-oxyethyldisulfanyl]ethyl 2-bromo-2- methylpropanoate ($(BiBOE)_2S_2$) (0.5 mM, dissolved with 15% ethanol) was cleaved with 0.5 M tris-(2-carboxyethyl)phosphine (TCEP) for 30 min at 37 °C, and connected to the AuNPs via the Au–S bond for 1 h at 37 °C [20]. Then after rinsing with 15% EtOH and ultrapure water, the electrodes were placed in 150 μL

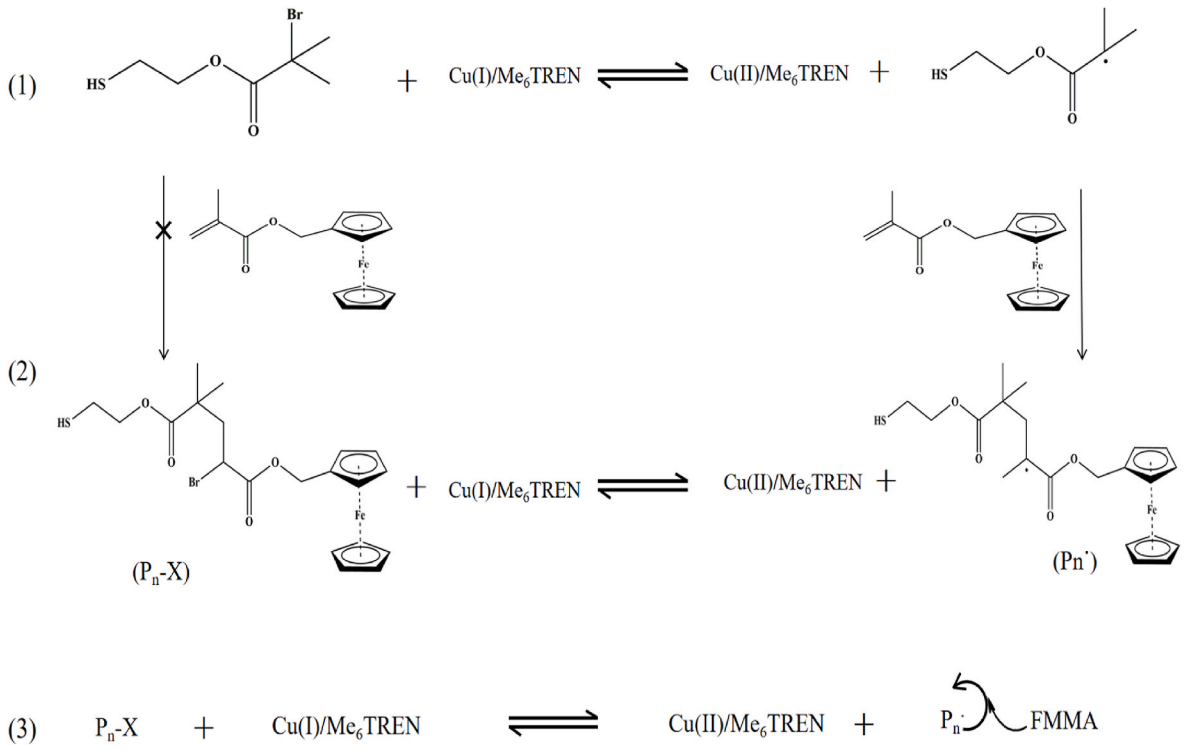

Scheme 2. The mechanism of AGET ATRP.

ferrocenylmethyl methacrylate (FMMA) monomer (10 mM, dissolved with DMF), 25 μL catalyst Cu(II)/Me_6TREN (10 mM, prepared by adding 6 μL Me_6TREN into 1 mL $CuBr_2$, dissolved with DMF), 50 μL ascorbic acid (AA) reductant (0.5 M, dissolve with Milli-Q water) and 275 μL DMF for ATRP reaction 1.5 h at 37 °C. Then 15% DMF and ultrapure water were used to wash the non-specifically adsorbed electroactive molecules on the electrode surface. Finally, the electrochemical biosensor was successfully prepared and ready for the square wave voltammetry (SWV) test in 0.5 M $LiClO_4$ solution.

3. Results and discussion

3.1. The principle of AGET ATRP reaction

As shown in Scheme 2, $(BiBOE)_2S_2$ was used as the initiator for the AGET ATRP system, and the Cu(II)/Me_6TREN complexes were reduced by the AA reductant to generate the activators Cu(I)/Me_6TREN complexes. Then Cu(I)/Me_6TREN could take the Br atom from $(BiBOE)_2S_2$ to form the high-oxidized metal halide Cu(II)/Me_6TREN and $(BiBOE)_2S_2$ was converted into free radical R•. Then R• initiated the polymerization of FMMA monomers to form chain growth radical P_n• (active species), P_n• can either continue to polymerize with the remaining monomer molecules or take Br atoms from Cu(II)/Br to form a temporarily inactivated macromolecular halide P_n-X (dormant species). The bromine

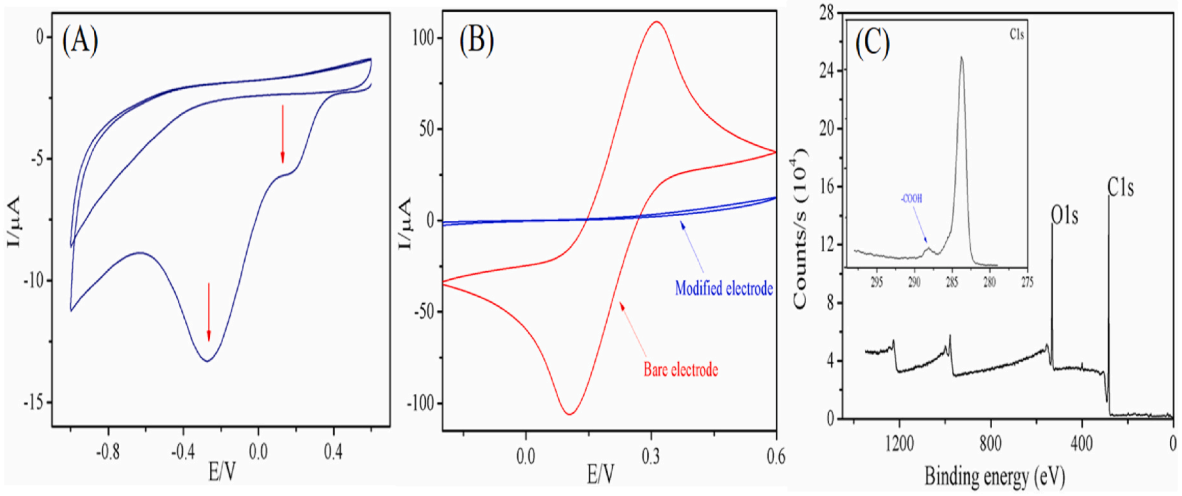

Fig. 1. (A) The CV of GCE in benzoic acid diazonium salt solution. (potential range: 0.6 to −1 V, scanning rate: 100 mV/s) **(B)** CVs of GCE before and after the modification of benzoic acid in a ferricyanide solution. **(C)** The XPS spectrum and carbon 1s high resolution spectrum (inset) of the benzoic acid modified GCE.

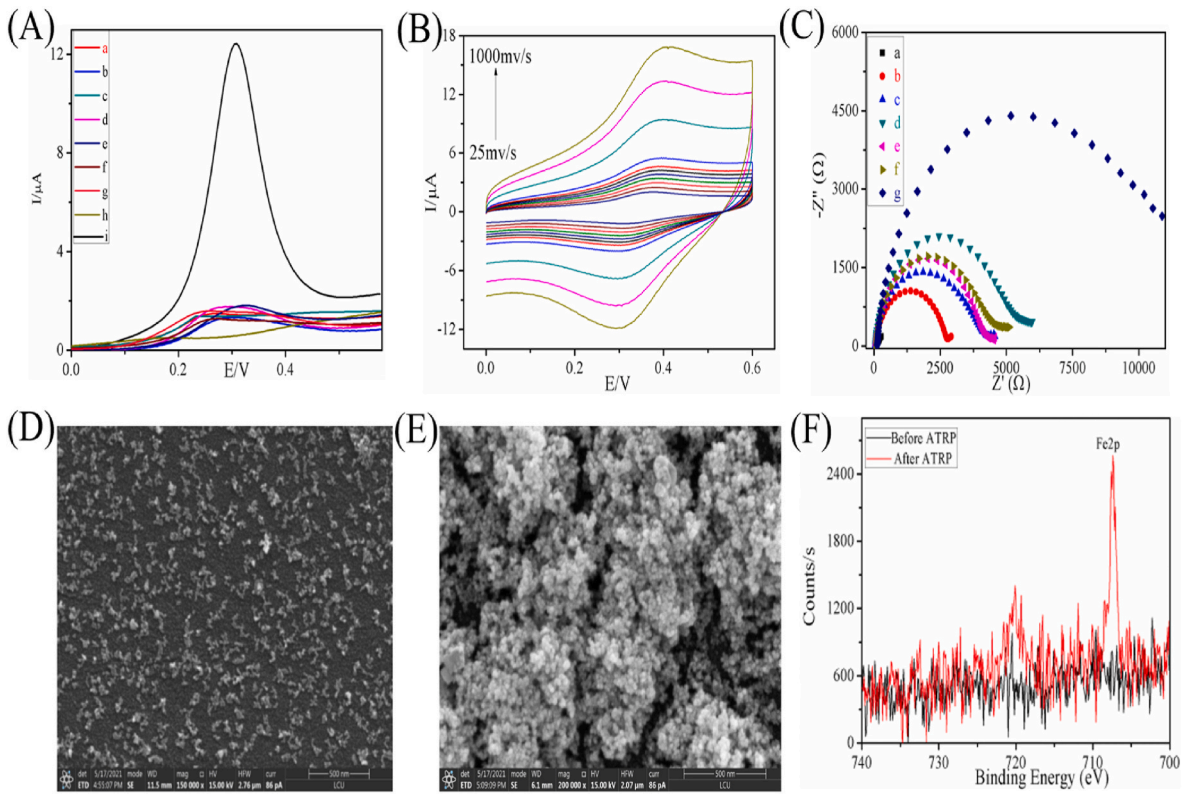

Fig. 2. (A) SWV of the benzoic acid/hairpin DNA/miRNA-141/AuNPs/initiator/FMMA polymer chain modified GCE (curve i), in the absence of benzoic acid (curve a), EDC/NHS (curve b), Hairpin DNA (curve c), miRNA-141 (curve d), AuNPs (curve e), initiator (curve f), AA (curve g), and FMMA(curve h). **(B)** CVs of benzoic acid/hairpin DNA/miRNA-141/AuNPs/initiator/FMMA polymer chain modified GCE at different scan rates. **(C)** EIS of the bare GCE (a), GCE modified with benzoic acid (b), benzoic acid/Hairpin DNA (c), benzoic acid/Hairpin DNA/miRNA-141 (d), benzoic acid/Hairpin DNA/miRNA-141/AuNPs (e), benzoic acid/hairpin DNA/miRNA-141/AuNPs/initiator (f), benzoic acid/hairpinDNA/miRNA-141/AuNPs/initiator/FMMA polymer chain (g). **(D)** The SEM image of the GCE surface before AGET ATRP reaction. **(E)** The SEM image of the GCE surface after AGET ATRP reaction. **(F)** XPS spectra of the electrode surface before and after AGET ATRP reaction.

atoms on P_n-Br can be taken away by Cu(I)/Me_6TREN again to produce the active species. Finally, polymers with a large quantity of FMMA can be obtained onto GCE surface by repeating the above AGET ATRP process, and the purpose of signal amplification detection of miRNA-141 was realized.

3.2. Ultraviolet–visible spectrum (UV–Vis) and transmission electron microscopy (TEM) characterizations of AuNPs

The AuNPs solution has a narrow ultraviolet–visible absorbance peak at 520 nm due to the surface plasmon resonance effect, which indicated that the AuNPs exhibited good dispersibility Fig. S1(A). TEM could observe the size and shape of the nanoparticles, as can be seen from Fig. S1(B), AuNPs were spherical particles with a diameter of about 15 nm. The particle size of AuNPs was further characterized by a particle size analyzer (Fig. S1(C)), which was consistent with the result of TEM analysis.

3.3. CV and XPS characterizations of the modified GCE

The electrochemical reduction of aryl diazonium salt is the most commonly used method for covalent derivatization of GCE surfaces [21–24]. As shown in Fig. 1(A), there were two characteristic peaks at the first sweep, the reduction peak of 0.16 V was the pre-enrichment process of *p*-carboxylic benzene molecule on the electrode surface, and the reduction peak around −0.26 V was the reduction peak of benzoic acid diazonium salt. These two reduction peaks disappeared completely in the second cycle, which proved that benzoic acid has been successfully modified to the GCE surface [25].

In Fig. 1(B), using $[Fe(CN)_6]^{3-}$/$[Fe(CN)_6]^{4-}$ as redox probes, CV was used to investigate the changes before and after benzoic acid modified electrode. It can be clearly seen that the oxidation and reduction peaks of ferricyanide were almost completely suppressed (blue curve) after the bare electrode (red curve) modified with benzoic acid. This strongly proved that the successful modification of benzoic acid impeded electron transfer on the surface of GCE. In addition, the surface of benzoic acid modified GCE was characterized by X-ray photoelectron spectroscopy. Fig. 1(C) shows the characteristic peaks of carbon 1s and oxygen 1s at 284 and 532 eV, respectively. The carbon 1s shows a peak at 288.8 eV, which was a typical characteristic peak of carboxylate group [24].

3.4. Feasibility analysis of the signal amplification strategy

Firstly, the feasibility of the proposed method was studied through SWV. It can be seen from Fig. 2(A), the GCE modified with benzoic acid/hairpin DNA/miRNA-141/AuNPs/initiator/FMMA polymer chain exhibited a strong oxidation peak at 0.3 V (curve i). This oxidation potential of Fc is consistent with the published literature [15]. However, in the process of preparing the sensor, GCE unmodified with benzoic acid (curve a), EDC/NHS (curve b), hairpin DNA (curve c), miRNA-141 (curve d), AuNPs (curve e), $(BiBOE)_2S_2$ initiator (curve f), reductant AA (curve g) and FMMA monomer (curve h) could be observed only very weak currents. Such a high signal-to-noise ratio proved the successful preparation of miRNA-141 biosensor. These results indicated that this signal amplification strategy can be used for highly sensitive electrochemical analysis of miRNA-141.

3.5. Electrochemical characterizations

In addition, the sensor was further characterized by CV. It can be

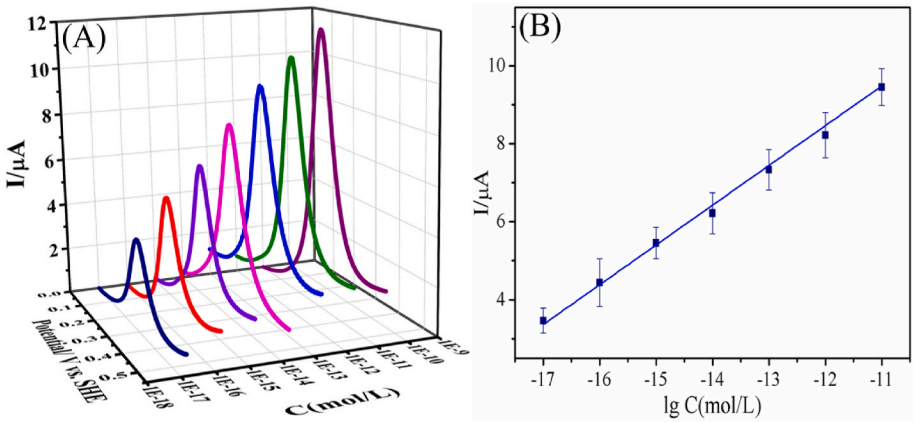

Fig. 3. (A) Electrochemical signal intensity measured by SWV at the concentration of target miRNA-141 in the range of 10 aM to 10 pM. **(B)** Calibration curve of the Fc oxidation current intensity versus the logarithm of miRNA-141 concentration.

seen from Fig. 2 (B) that as the scan rate increased, the peak currents of the oxidation peak and reduction peak increased and decreased, respectively. There was a good linear relationship between the peak current and the scanning speed, which indicated that the formation process of Fc polymer was surface-confined. The linear equations and graphs (Fig. S2) were presented in the *supplementary materials*.

Electrochemical impedance spectroscopy (EIS) was used to characterize the gradual establishment process of electrochemical sensor. It can be seen from Fig. 2 (C) that the resistance of bare electrode was small (curve a). After modified with benzoic acid, the resistance of the GCE was increased due to the low solubility and poor electrical conductivity of benzoic acid (curve b). When the hairpin DNAs were immobilized on the benzoic acid modified GCE surface through amidation reaction, the electronegative phosphate groups of hairpin DNAs had electrostatic repulsion to $[Fe(CN)_6]^{3-/4-}$, which made it far away from the electrode surface and further increased the resistance (curve c). The target miRNA-141 was captured by the hairpin DNA probe, the resistance was further increased (curve d). Interestingly, when AuNPs were covalently attached to the ends of the hairpin DNAs, the resistance decreased (curve e). This may be due to the fact that AuNPs promoted electron transfer to some extent. After connected with initiator, the resistance increased slightly (curve f). Finally, after the polymerization reaction, the resistance significantly increased (curve g), which indicated that a great amount of highly hydrophobic polymers was produced on the GCE surface to hinder the electron transfer of probe molecules. These results also revealed the successful preparation of the sensor. It is important to note that although the formed polymer is electroactive (the Fc probe has redox activity), due to the electrons on the polymer skeleton are not delocalized, the hydrophilic $[Fe(CN)_6]^{3-/4-}$ was extruded from the GCE surface, resulting in a significant increase of resistance.

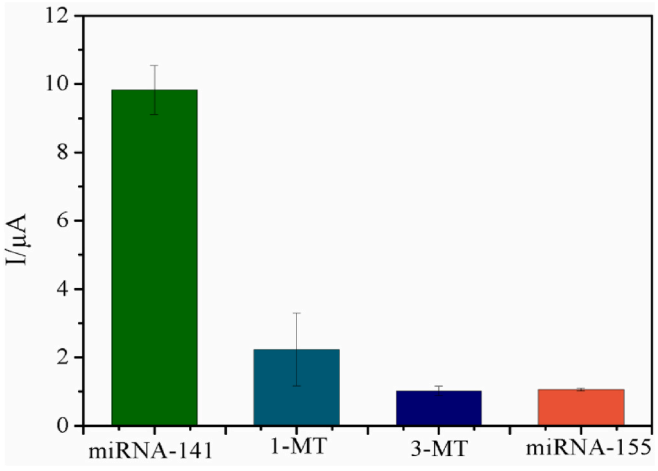

Fig. 4. Specificity of the assay for microRNA-141(10 pM) against other miRNAs (the concentration of 1-MT, 3-MT and miRNA-155 were 1 nM).

3.6. SEM and XPS characterizations

In order to better prove the successful preparation of the sensor and the polymerization of signal molecules through AGET ATRP reaction. SEM and XPS were used to respectively characterize the morphology and elemental changes of the electrode surface before and after the polymerization reaction. Fig. 2(D) is the SEM image of electrode surface before AGET ATRP reaction, only small particles of AuNPs were observed on the electrode surface. While after AGET ATRP reaction, it can be clearly seen from Fig. 2 (E) that polymers were formed on the electrode surface. As shown in Fig. 2 (F), the XPS characterization explained the element changes before and after AGET ATRP reaction. The XPS peak of Fe element was not observed before polymerization, while it appeared at 707.6 eV after the AGET ATRP reaction, indicating that FMMA monomers were successfully polymerized via AGET ATRP reaction.

3.7. Optimization of experimental conditions

The experimental conditions which might affect the sensor signal have been optimized. As shown in Fig. S3 (A), the optimal dosage of FMMA monomer was 150 μL. The function of AA was to reduce the high-value metal Cu(II) to the low-value metal catalyst Cu(I), so the dosage of the reductant AA has been optimized. Fig. S3 (B) shows the optimal dosage of AA was 50 μL. Subsequently, the Me_6TREN ligand was used to increase the solubility of metal catalysts in the reaction system. The result shows (Fig. S3 (C)) the optimal dosage was 6 μL. Finally, the growth of the polymer was accompanied by continuous enrichment of the electroactive probe on GCE surface. As shown in Fig. S3 (D), the oxidation current increased rapidly with the extension of ATRP time and tended to be stable after 90 min, so the polymerization time was selected at 90 min.

3.8. Electrochemical detection of miRNA-141

Under the optimal conditions, the prepared sensors were placed in 0.5 M $LiClO_4$ for SWV experiment. As shown in Fig. 3(A), as the concentration of the target miRNA-141 increased, the oxidation peak current of the signal molecule Fc also increased. The peak current had a good linearity with concentration in the range of 10 pM - 10 aM, and the linear regression equation was I (μA) = 0.98lgC + 20.09 (R^2 = 0.9979).

Table 1
The determination of miRNA-141 in human serum samples.

Samples	Found	Added	Total Found	RSD % (n = 3)	Recovery
1	30 aM	0.1 fM	0.14 fM	3.84	110%
2	0.11 fM	10 fM	9.91 fM	7.46	98%
3	0.17 fM	1pM	1.07 pM	14.12	106.9%

The limit of detection (LOD) was estimated to be 3.23 aM (S/N = 3). Briefly, the average value of the signal generated by 11 times control groups was the noise (N), and then 3 times of N was put into the linear equation, the calculated concentration C was LOD. In addition, LODs obtained by other sensors for detection of miRNA-141 were listed in Table S2. Obviously, compared with other methods, our signal amplification strategy exhibited a higher sensitivity with a lower LOD.

3.9. Selectivity and stability of the biosensor

The selectivity of biosensor is an important index to evaluate the performance of a sensor. Therefore, in the process of target recognition, single base mismatch target (1 MT), three base mismatch target (3 MT) and miRNA-155 were used as interferences to replace the target miRNA-141 for complementary pairing with the hairpin DNA, and the SWV responses of the sensors were measured. As depicted in Fig. 4, the electrochemical signal of miRNA-141 was 4.5, 8.8 and 8.7 times higher than that of 1 MT, 3 MT and miRNA-155, respectively. These results indicated that the prepared biosensor had good specificity for the highly sensitive electrochemical detection of miRNA-141.

In addition, the stability of the sensor was also evaluated. Ten GCE electrodes of the same batch were divided into two groups after the same treatment. After the ATRR reaction, the first group was subjected to the SWV test, the second group was stored in a refrigerator at 4 °C and performed the SWV test after a week. The experimental results showed that the average oxidation peak current of the second group is 9.3% lower than that of the first group, which indicated that the electrochemical sensor had good stability.

4. Application in serum sample for miRNA-141 analysis

To evaluate the reliability and application potential of the sensor in real serum samples, the prepared sensor was tested by a standard addition method for sample analysis. Healthy human serum (purchased from Beijing Solarbio Science & Technology Co., Ltd.) was diluted 10 times. The addition amount of target miRNA-141 was 10 aM, 10 pM and 10 fM. As seen from Table 1, the sample recovery rate was in the range of 98–106.9%. The experimental results indicated that the proposed biosensor had an excellent potential for clinical analysis of miRNA-141.

5. Conclusions

In summary, an electrochemical sensor based on AGET ATRP signal amplification for sensitive and selective analysis of miRNA-141 was successfully constructed. Different from conventional amplification strategies, this method has no requirements for enzymes or complex nanomaterials. Results showed that this proposed electrochemical biosensor had higher sensitivity than the other ones, and it could realize the miRNA-141 analysis in real serum samples and obtain satisfactory results. Moreover, this signal amplification method offered a new strategy for highly sensitive analysis of other miRNA, which possesses great significance in disease diagnosis.

Declaration of competing interest

The authors declare that they have no known competing financial interests or personal relationships that could have appeared to influence the work reported in this paper.

Acknowledgements

This work was financially supported by the National Natural Science Foundation of China (No. 21974068, 21890740, 21890742 and 9195401).

Appendix A. Supplementary data

Supplementary data to this article can be found online at https://doi.org/10.1016/j.talanta.2021.122744.

References

[1] R.M. Graybill, R.C. Bailey, Emerging biosensing approaches for microRNA Analysis, Anal. Chem. 88 (2016) 431–450, https://doi.org/10.1021/acs.analchem.5b04679.
[2] H.F. Dong, J.P. Lei, L. Ding, Y.Q. Wen, H.X. Ju, X.J. Zhang, MicroRNA: function, detection, and bioanalysis, Chem. Rev. 113 (2013) 6207–6233, https://doi.org/10.1021/cr300362f.
[3] S.P. Song, Y. Qin, Y. He, Q. Huang, C.H. Fan, H.Y. Chen, Functional nanoprobes for ultrasensitive detection of biomolecules, Chem. Soc. Rev. 39 (2010) 4234–4243, https://doi.org/10.1039/C000682N.
[4] J.J. Xu, W.W. Zhao, S.P. Song, C.H. Fan, Functional nanoprobes for ultrasensitive detection of biomolecules: an update, Chem. Soc. Rev. 43 (2014) 1601–1611, https://doi.org/10.1039/c3cs60277j.
[5] H.F. Dong, J.P. Lei, L. Ding, Y.Q. Wen, H.X. Ju, X.J. Zhang, MicroRNA: function, detection, and bioanalysis, Chem. Rev. 113 (2013) 6207–6233, https://doi.org/10.1021/cr300362f.
[6] J.L. Liu, Z.L. Tang, Y. Zhuo, Y.Q. Chai, R. Yuan, Ternary electrochemiluminescence system based on rubrene microrods as luminophore and Pt nanomaterials as coreaction accelerator for ultrasensitive detection of microRNA from cancer cells, Anal. Chem. 89 (2017) 9108–9115, https://doi.org/10.1021/acs.analchem.7b01812.
[7] Z.Y. Li, Z.F. Lin, X.Y. Wu, H.T. Chen, Y.Q. Chai, R. Yuan, Highly efficient electrochemiluminescence resonance energy transfer system in one nanostructure: its application for ultrasensitive detection of microRNA in cancer cells, Anal. Chem. 89 (2017) 6029–6035, https://doi.org/10.1021/acs.analchem.7b00616.
[8] Y.H. Liao, Y. Fu, Y.X. Wu, R. Huang, X.M. Zhou, D. Xing, Ultrasensitive detection of microRNA in tumor cells and tissues via continuous assembly of DNA probe, Biomacromolecules 16 (2015) 3543–3551, https://doi.org/10.1021/acs.biomac.5b00959.
[9] H.L. Shao, J. Lu, Q.Q. Zhang, Y.F. Hu, S.Wang, Z. Y. Guo, Ruthenium-based metal organic framework (Ru-MOF)-derived novel Faraday-cage electrochemiluminescence biosensor for ultrasensitive detection of miRNA-141, Sensor. Actuator. B Chem. 268 (2018) 39–46, https://doi.org/10.1016/j.snb.2018.04.088.
[10] H.V. Tran, B. Piro, S.Reisberg, L. D. Tran, H. T. Duc, M. C. Pham, Label-free and reagentless electrochemical detection of microRNAs using a conducting polymer nanostructured by carbon nanotubes: application to prostate cancer biomarker miR-141, Biosens. Bioelectron. 49 (2013) 164–169, https://doi.org/10.1016/j.bios.2013.05.007.
[11] M.J. Li, W.B. Liang, R.Yuan, Y. Q. Chai, CdTe QD-CeO_2 complex as a strong photoelectrochemical signal indicator for the ultrasensitive microRNA assay, ACS Appl. Mater. Interfaces 11 (2019) 11834–11840, https://doi.org/10.1021/acsami.9b0218910.1021/acsami.9b02189.s001.
[12] C. Wang, Q. Han, F.J. Mo, M. Chen, Y.Z. Fu, Novel luminescent nanostructured coordination polymer: facile fabrication and application in electrochemiluminescence biosensor for microRNA-141 Detection, Anal. Chem. 92 (2020) 12145–12151, https://doi.org/10.1021/acs.analchem.0c00130.
[13] Z.H. Xu, H. Wang, J. Wang, W. Zhao, J.J. Xu, H.Y. Chen, Bidirectional electrochemiluminescent sensing: an application in detecting miRNA-141, Anal. Chem. 91 (2019) 12000–12005, https://doi.org/10.1021/acs.analchem.9b02914.
[14] H.B. Sun, L.S. Qian, J.M. Kong, X.J. Zhang, Ultra-sensitive nucleic acid detection based on target cycling of triple helix molecular switch and ATRP double signal amplification, Sensor. Actuator. B Chem. 337 (2021) 129–791, https://doi.org/10.1016/j.snb.2021.129791.
[15] A.J.D. Magenau, N.C. Strandwitz, A. Gennaro, K. Matyjaszewski, Electrochemically mediated atom transfer radical polymerization, Science 332 (2011) 81–84, https://doi.org/10.1126/science.1202357.
[16] B. Li, B. Yu, W.T.S. Huck, F. Zhou, W.M. Liu, Electrochemically induced surface-initiated atom-transfer radical polymerization Angew, Chem. Int. 51 (2012) 5092–5095, https://doi.org/10.1002/ange.201201533.
[17] S. Kim, H.D. Sikes, Radical polymerization reactions for amplified biodetection signals, Polym. Chem. 11 (2020) 1424–1444, https://doi.org/10.1039/C9PY01801H.
[18] X.L. Peng, H.L. Yan, Z. Wu, W. Wen, X.H. Zhang, S.F. Wang, Magnetic Nanobeads and de novo growth of electroactive polymers for ultrasensitive microRNA detection at the cellular level, Anal. Chem. 93 (2021) 902–910, https://doi.org/10.1021/acs.analchem.0c03558.
[19] Y. Yeh, B. Creran, V. Rotello, Gold nanoparticles: preparation, properties, and applications in bionanotechnology, Nanoscale 4 (2012) 1871–1880, https://doi.org/10.1039/c1nr11188d.

[20] N.J. Warren, C. Muise, A. Stephens, S.P. Armes, A.L. Lewis, Near-monodispersepoly (2-(methacryloyloxy)ethylphosphorylcholine)-based macromonomer prepared by atom transfer radical polymerization and thiol-ene click chemistry: novel reactive steric stabilizers for aqueous emulsion polymerization, Langmuir 28 (2012) 2928–2936, https://doi.org/10.1021/la204083z.

[21] P. Allongue, M. Delamar, B. Desbat, O. Fagebaume, R. Hitmi, J. Pinson, J. M. Saveant, Covalent modification of carbon surfaces by aryl radicals generated from the electrochemical reduction of diazonium Salts, J. Am. Chem. Soc. 119 (1997) 201–207, https://doi.org/10.1021/ja963354s.

[22] G.Z. Liu, T. Böcking, J.J. Gooding, J. Diazonium salts: stable monolayers on gold electrodes for sensing applications, J. Electroanal. Chem. 600 (2007) 335–344, https://doi.org/10.1016/j.jelechem.2006.09.012.

[23] S. Eissaa, N. Alshehria, A.M. Rahmana, M. Dasouki, K.M. Abu-Salah, M. Zourob, Electrochemical immunosensors for the detection of survival motor neuron (SMN) protein using different carbon nanomaterials-modified electrodes, Biosens. Bioelectron. 101 (2018) 282–289, https://doi.org/10.1016/j.bios.2017.10.015.

[24] S. Ranganathan, I. Steidel, F. Anariba, R.L. McCreery, Covalently bonded organic monolayers on a carbon substrate: a new paradigm for molecular electronics, Nano, Letture 1 (2001) 491–494, https://doi.org/10.1021/nl015566f.

[25] Y.C. Liu, R.L. McCreery, Reactions of organic monolayers on carbon surfaces observed with unenhanced Raman spectroscopy, J. Am. Chem. Soc. 117 (1995) 11254, https://doi.org/10.1021/ja00150a024.